Effect of the pouring temperature by novel synchronous rolling-casting for metal on microstructure and properties of ZLl04 alloy

Xiaoqiang Luo[a)]
Department of Inorganic Nonmetallic Materials, School of Materials Science and Engineering, University of Science and Technology Beijing, Beijing, China; and Key Lab of Mechanics in Advanced Manufacturing, Institute of Mechanics, Chinese Academy of Sciences, Beijing, China

Qingzhi Yan
Department of Inorganic Nonmetallic Materials, School of Materials Science and Engineering, University of Science and Technology Beijing, Beijing, China

Zhengyang Li
Key Lab of Mechanics in Advanced Manufacturing, Institute of Mechanics, Chinese Academy of Sciences, Beijing, China

(Received 27 March 2016; accepted 1 June 2016)

A novel synchronous rolling-casting for metal (SRCM) process for producing metal components is developed. In this paper, the microstructure evolution and mechanical property of ZLl04 alloy with different pouring temperatures by SRCM are investigated. In the process, the pouring temperature has great effects on the microstructure and mechanical property primarily through the crystal change in the rolling-casting area. Temperature of liquids and solids of ZL104 alloy is measured by differential scanning calorimetry. Distribution and characteristics of the microstructure of samples are examined by optical microscopy, scanning electron microscopy equipped with energy dispersive spectrometer. The results show that the samples fabricated by SRCM present uniform structure and good performance with the pouring temperature at 620 °C when the velocity of the substrate is at 10 cm/s. The tensile strength of ZLl04 alloy reaches 211.89 Mpa, while the average vickers hardness is 81.5 HV.

I. INTRODUCTION

Synchronous rolling-casting for metal (SRCM) is a novel direct manufacturing processing technology translating virtual solid model data into products in a layer by layer process. SRCM has aroused many attentions due to its short period of processing products with complicated shape and high performance.[1–4]

In the field of additive manufacturing, researchers usually fabricate the metal final parts or near-net parts by fusing wire or powder of raw materials and combining the liquid metal layer by layer. M. Orme developed the way of droplets without mold in 1990s,[5] and C. R. Rice put forward the semisolid slurry process without mold in 2000.[6] C. R. Deckard proposed the selective laser sintering. A laser is used to selectively bind a layer of powder and continuously a new layer of powder is swept over the top of the previous layer after the completion of each layer.[7,8] C. W. Hull proposed the stereo lithography, in which substrate is lowered layer by layer into a vat of photopolymer liquid. At each layer, the photopolymer is selectively exposed to light, causing hardening of the region and thus defines the part.[9] S. S. Crump brought fused deposition modeling, which separately deposits both the part and support materials.[10,11] Laser engineered net shaping, known as LENS, uses high energy laser beam to form and move a partial melting of molten pool; meanwhile, the metal powder or wire were poured synchronously into the molten pool. Therefore metallurgical combination of cladding is formed after cooling section, and metal components with high density are prepared by cladding step by step.[12–14]

Recently, the slurry course of aluminum alloys with better mechanical properties compared to parts made by conventional casting had been used for the fabrication of parts without mold molding method and attracted the attentions of scholar, using the merit of semisolid slurry forming processing.[15–17] SRCM is a pioneering metal processing technology. The finished liquid metal is pressed out from the outlet of base of crucible with a horizontal movable plate assembled near the outlet. With the aid of 3D software, the melted metal is solidified and formed layer by layer. The technology has gathered the parts of design, processing, and molding, reduced the sophisticated processing equipment and energy consumption, and had broad application prospects. For this reason, they are well suited to the aerospace, the automobile industry and other fields, etc.[18]

Contributing Editor: Jürgen Eckert
a)Address all correspondence to this author.
e-mail: lxq.5566@163.com
DOI: 10.1557/jmr.2016.233

In this work, ZL104 alloy was prepared by SRCM. In the preparation process, effects of the pouring temperature by SRCM on microstructure and mechanical property of ZLl04 alloy had been studied. The results show that the samples fabricated by SRCM display a uniform structure and good performance with the pouring temperature at 620 °C and the velocity of the substrate at 10 cm/s. The tensile strength of ZLl04 alloy reaches 211.89 Mpa, while the average vickers hardness reaches 81.5 HV.

II. EXPERIMENTS

A. The principle of SRCM

The process principle of SRCM is shown in Fig. 1. It consists of a heating system with a crucible, heating furnace, and a movable plate. During the process of such technique, liquid metal is stirred uniformly and vertically pressured though a nozzle to a rolling-casting zone, an open flat space between the nozzle and the plate with diameter in millimeters and thickness in millimeters. Meanwhile, the plate, served as crystallizer and cooler, moving horizontally in a withdrawn out of the rolling-casting zone. By means of 3D controlling system, liquid metal is filled and solidified in given patterns layer by layer, and then a metal part is formed. Between the discharging mouth and metallurgical combination, the metallic melts begin to solidify rapidly, and the dendrite formed rapidly by supercool brought by this solidification process. Hence, the pouring temperature takes great effects on the slurry of metals.

B. Material

In this experiment, a commodity ZL104 aluminum silicon cast alloy was used; the chemical composition of ZL104 alloy investigated is listed in Table I. The density was 2.71 kg/m^3.

C. Alloy preparation

To obtain fine and globular microstructure, the ZL104 aluminum silicon alloys were heated to a temperature between liquids and solidus zone which is sufficient condition required for the forming. In this experiment, we choose the pouring temperature at different temperatures with the velocity of the substrate at 10 cm/s; the pouring temperature is higher than that of the nozzle. The samples for microstructure observation were prepared by standard metallographic techniques. For microstructures, observation samples were cut off from the quenched slurries, roughly ground, and polished and etched by an aqueous solution of 0.5% HF for 15 s. The etched samples were cleaned with an alcohol and dried, then analyzed by optical microscopy (OM), and the representative microstructure of the slurry can be obtained. All the metallographic samples were examined by OM, scanning electron microscopy (SEM), and energy dispersive spectrometer (EDS). T1 thermal treatment of the samples involved artificial aging. Figure 2 shows the schematic drawing of the sample location for ZL104 aluminum silicon cast alloy microstructure analysis.

Therefore, this window of heated temperature could be controlled within liquids temperatures and solidus temperatures to get a proper solid fraction and a proper degree of superheat, the sample of ZL104 alloy for tensile test is shown as Fig. 3.

TABLE I. The composition of ZL104 (wt%).

Si	Fe	Mn	Zn	Mg	Ni	Cu	Al
9.3	0.60	0.35	0.25	0.25	0.2	0.1	Bal.

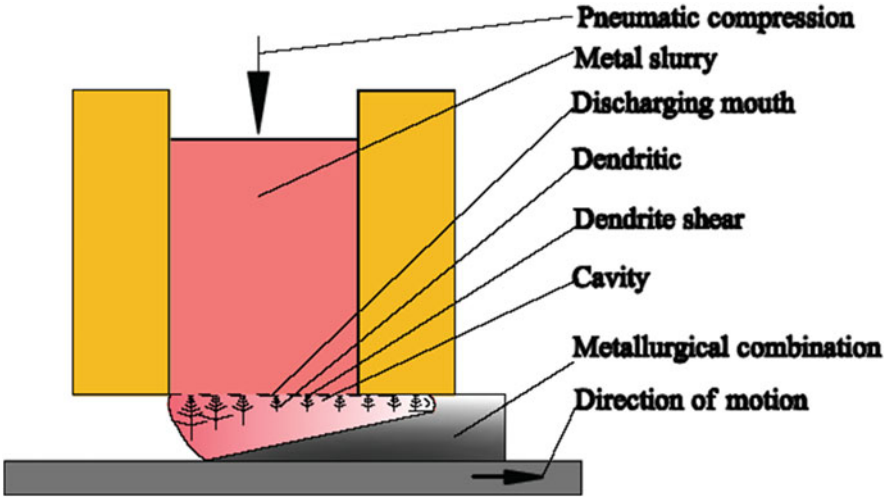

FIG. 1. SRCM equipment.

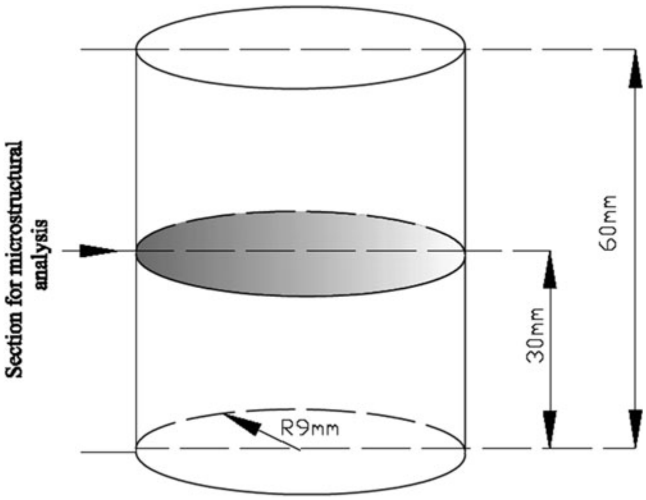

FIG. 2. The sample location for semisolid microstructure analysis.

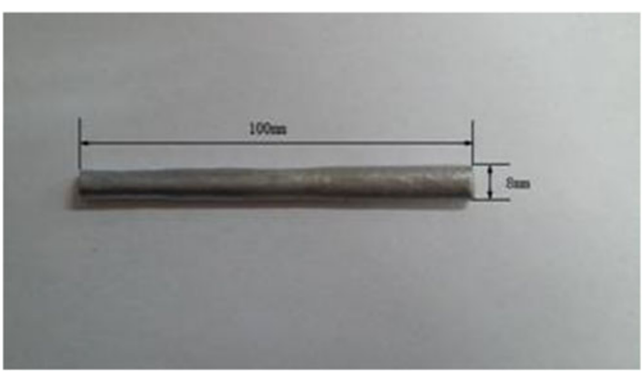

FIG. 3. Typical metal part made by synchronous rolling-casting.

D. Testing methods

The average grain size was calculated by

$$D = L_f/(N_f * \mu) \quad . \tag{1}$$

The D is the average grain size, L_f is the length of measure line, N_f is the grain count that is covered by the measure line and μ is the magnification value.

The average roundness of the grain shape was calculated by

$$S = L_P^2/(4\pi A_P) \quad . \tag{2}$$

The S is the average roundness, L_P and A_P are total circumference of measure grains and grain areas value of globule, respectively. The average roundness of the grain shape was calculated by image analysis software.

ZL104 cast alloy has been used for fabricating tensile samples. The tensile samples for mechanical property tests were obtained from middle region, the samples were machined to specimens shown in Fig. 4, and the tensile test was carried out by a CMT5105 tensile

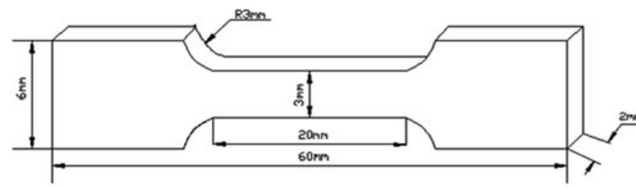

FIG. 4. Schematic illustration of tensile test.

machine (MTS Industrial Systems Co. Ltd., Shenzhen, China), the results of the tensile tests reported in this work were the average obtained from five tensile test specimens. The hardness was test by a XHB-3000 Brilled durometer (Shanghai Everone Precision Instrument Co. Ltd., Shanghai, China). The samples were conducted by using a 62.5 kg load and 5 mm diameter indentor, and the loading time was about 30 s.

III. RESULTS AND DISCUSSION

A. Differential scanning thermal analysis

The commodity ZL104 aluminum silicon cast alloy was heated to 700 °C at 5 °C/min and cooled to room temperature. The heat flow and temperature were tested with a K-type thermocouple to obtain differential scanning calorimetry (DSC) curves as shown in Fig. 5. Obvious endothermic process occurred at point A in ZL104 alloy, the endothermic process is over at point C; it shows that the solidus and liquidus temperatures of this alloy were 571.2 °C and 604.1 °C, respectively.

B. Effects of the pouring temperature on the microstructure and mechanical property of the ZL104 alloy

Figure 6 shows backscattered electron (BSE) image and EDS spectra of the sample with two regions of ZL104 aluminum alloys which exhibits typical dendritic microstructure, furthermore, it is found from BSE image that white needle-shaped precipitates is Si (point 1), the gray precipitates is α-Al (point 2), the shine precipitates is $AlSi_9Mg$, and the microstructure of ZL104 alloy is mainly composed of matrix α-Al and eutectic Si phase. According to the EDS results of ZL104 aluminum alloy, it is confirmed that arrow "1" (white needle-shaped precipitates) and the arrow "2" (gray precipitates) in Fig. 6 are eutectic Si and eutectic α-Al phases, respectively. It is found from Fig. 6 that the ZL104 aluminum alloy has microstructure in complex irregular shape, the Si phase is needle-shaped, and the α-Al is gray precipitates alloy mainly exhibiting a large block shape.

During the SRCM process, in preparation of metallic melts for synchronous rolling-casting using the temperature control and mixing system, the dendrite become short grain under the action of shear force in the areas of rolling-casting. Figure 7 shows the optical microstructure images of

four kind of samples with different pouring temperatures at the rolling-casting process at 10 cm/s. Figure 7(a) is the ZL104 aluminum alloy with pouring temperature at 580 °C, Fig. 7(b) is the pouring temperature at about 600 °C, Fig. 7(c) is the pouring temperature at about 620 °C, and Fig. 7(d) is the pouring temperature at about 640 °C. The four samples are high temperature molded without cold working besides cooling (T1 state). The process of SRCM is focused on solidification and melting. The pouring temperature with movement speed of base plate made the dendrite become short grain under the action of shear force, so as to achieve the goal of fine grains. The process enables molten to pile up layer by layer along the height direction into a complex model. Metallic melts rapidly forms dendrite between the mouth and crystallization plate cavity synchronous casting-rolling area. The pouring temperature at 620 °C and substrate speed at 8 cm/s has a uniform microstructure and there is very few dendritic.

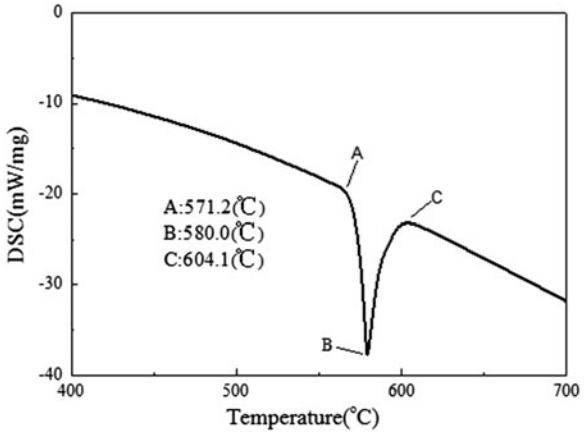

FIG. 5. DSC curve of ZL104.

Figure 8 shows the SEM of four samples. Figure. 8(a) is the ZL104 aluminum alloy with pouring temperature at 580 °C, Figs. 8(b)–8(d) is the pouring temperature controlled at 600 °C, 620 °C, 640 °C, respectively, with the velocity of the substrate at 8 cm/s. The samples are high temperature molded without cold working besides cooling (T1 state), the grain becomes more rounded with the appropriate pouring temperature. It was proved that dendrite breakage and nucleation were the main reasons of fine spherical microstructure formation, pouring temperature combination with shearing strength can affect the dendrite fusing of the melt. The rolling-casting speed affects grain shape, but its impact on grain size is not obvious, the experimental with the pouring temperature at 620 °C and substrate speed at 10 cm/s has a uniform microstructure and there is very few dendritic. Obviously, the pouring temperature at 640 °C and 580 °C has segregation, respectively.

Figure 9 shows the relationships between the rolling-casting temperature, average roundness and average grain

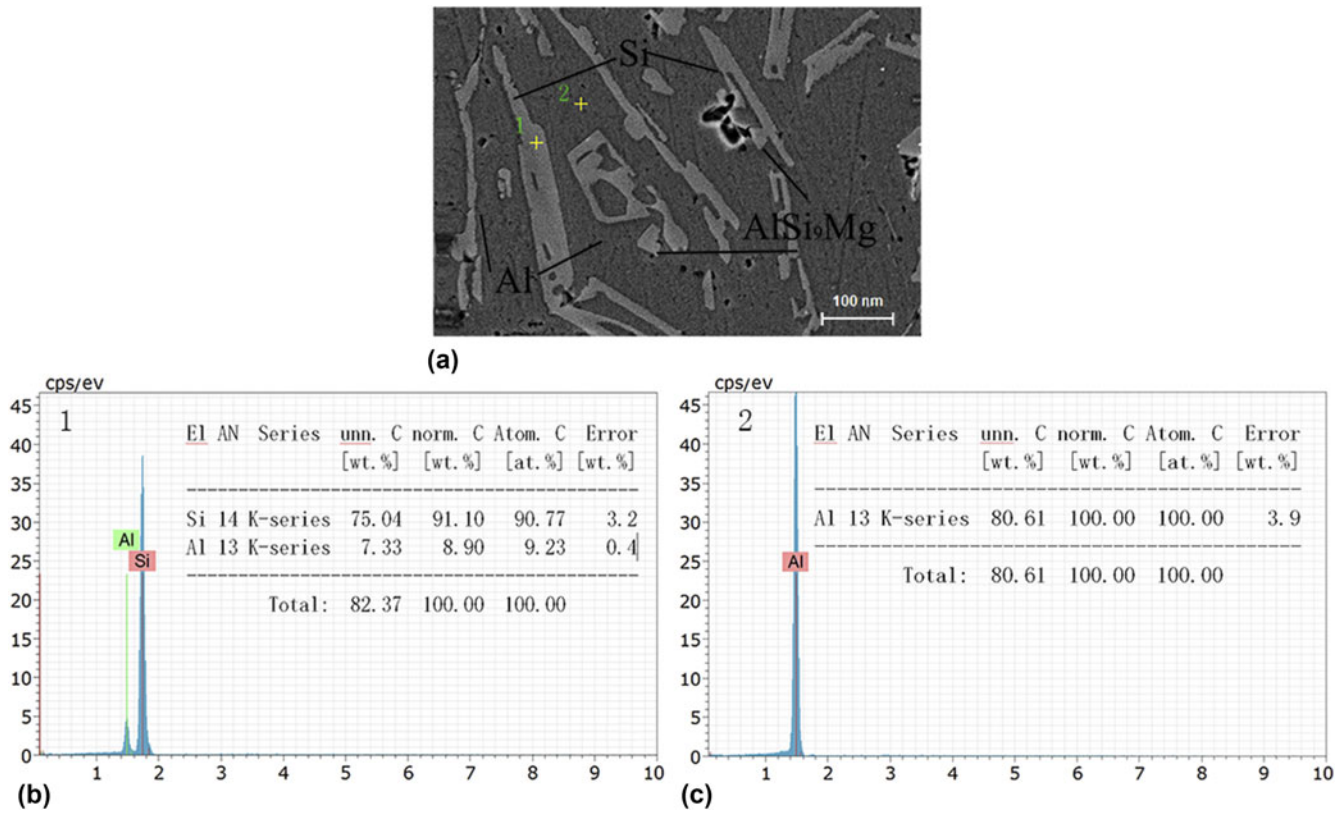

FIG. 6. BSD image of ZL104 alloy samples. (a) BSD image; (b), (c) the energy spectrum test region with the EDS results.

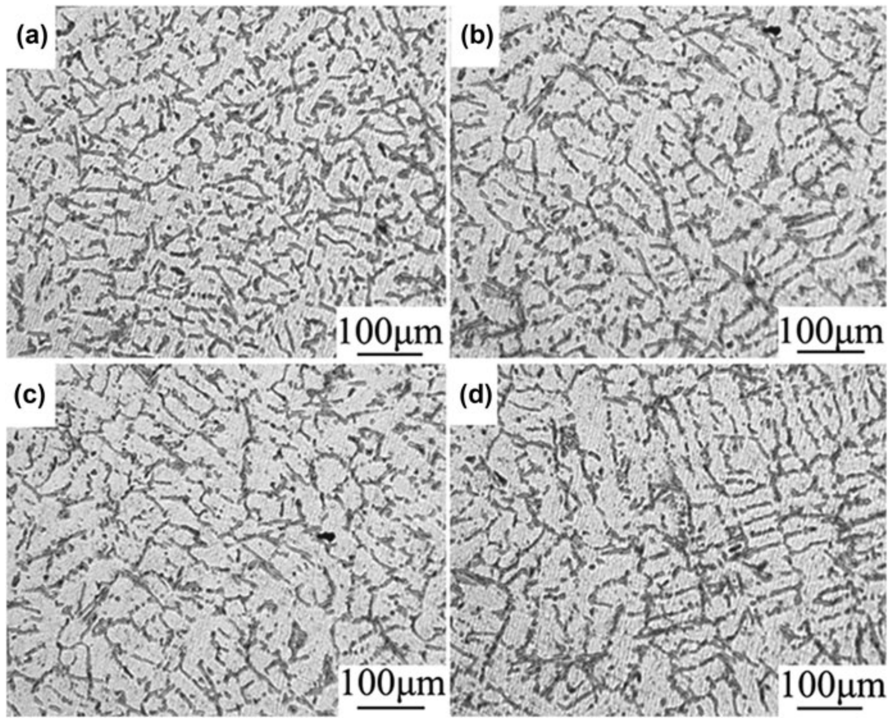

FIG. 7. OM images of the ZL104 experimental alloy treated at different pouring temperatures. (a) 580 °C, (b) 600 °C, (c) 620 °C, and (d) 640 °C.

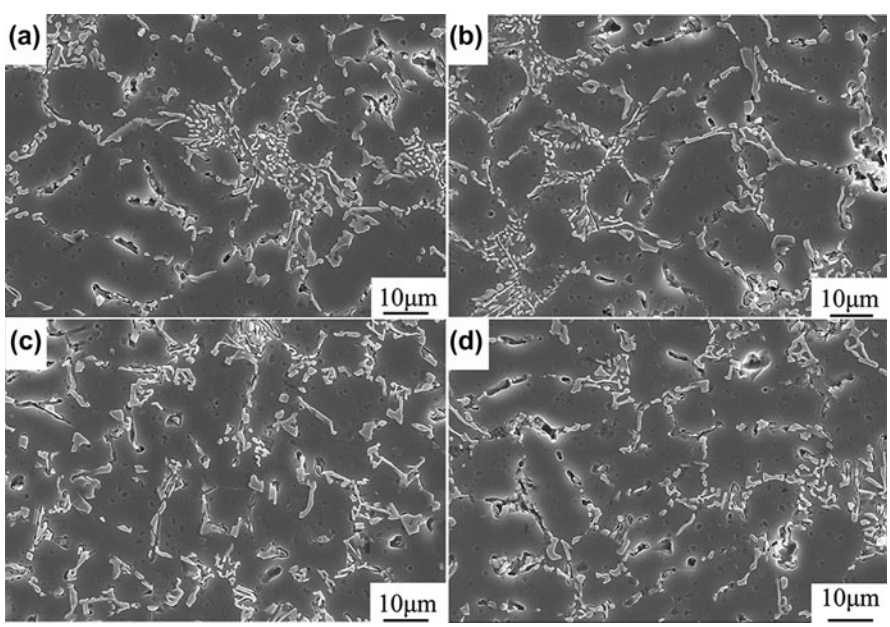

FIG. 8. SEM images of the ZL104 experimental alloy treated at different pouring temperature. (a) 580 °C, (b) 600 °C, (c) 620 °C, and (d) 640 °C.

size. The primary grain size is best developed at pouring temperature at 620 °C, the rolling-casting temperature can affect the nucleation rate and shearing strength of the melt in the rolling-casting zones, and further influence the final grain size of the ZLl04 alloy. The nucleation rate decreased with the temperature increasing and decreasing from 620 °C. Furthermore, the liquid fraction of the ZLl04 slurry increased with the increasing increments of the casting temperature, and viscosity decreased correspondingly. As stated, the shearing force in the melt is determined by the substrate movement speed and viscosity, so the shearing strength reduces with the decrease of the viscosity of ZLl04 slurry. For this reason, a high rolling-casting temperature could have caused a weak shearing strength and low nucleation rate, which caused coarse dendrite formation. When the rolling-casting

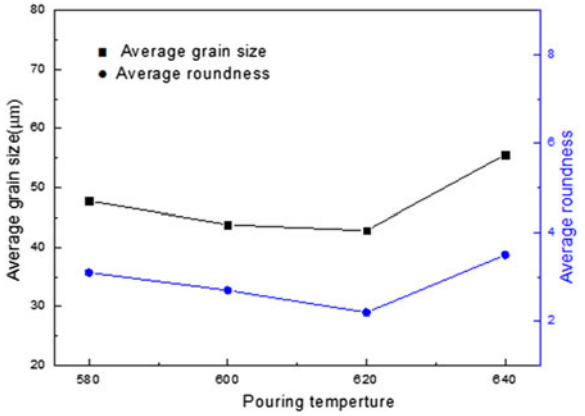

FIG. 9. The average grain size and roundness at different pouring temperatures.

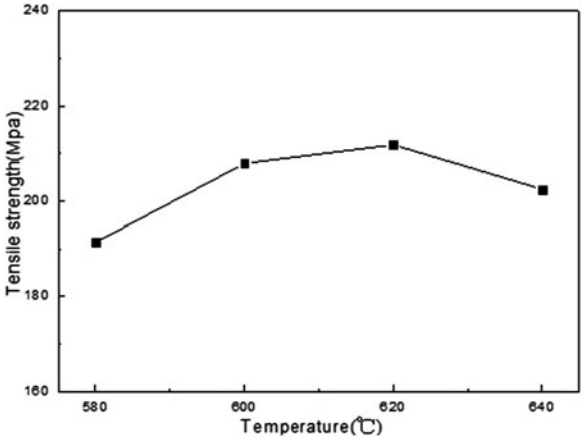

FIG. 10. SEM images of the ZL104 experimental alloy treated at different pouring temperatures.

temperature was between 600 °C and 640 °C, many obvious big dendrites formed in the microstructures of the ZLl04 slurry, as shown in Figs. 7(b) and 7(d). On the other side, the shearing strength increased and nucleation rate with the decrease of the rolling-casting temperature, and the roundness and grain size decreased, respectively, as shown in Figs. 7(a) and 7(b). Nevertheless, if the rolling-casting temperature was lower than 580 °C, the melt flow ability of the ZLl04 slurry was very poor, and the operation procedure usually failed. For these reasons, we suggest a reasonable rolling-casting temperature to be 620 °C.

Between the mouth and crystallization plate cavity area of synchronous, the metallic melts begin to solidification rapidly, the dendrite rapid formation by metallic melts, in the process the pouring temperature take great effect on the slurry of metals.

C. Microstructure and properties of the ZL104 alloy produced by the process

At a velocity of plate at 10 cm/s and the rolling-casting temperature at 580 °C, 600 °C, 620 °C, and 640 °C, four

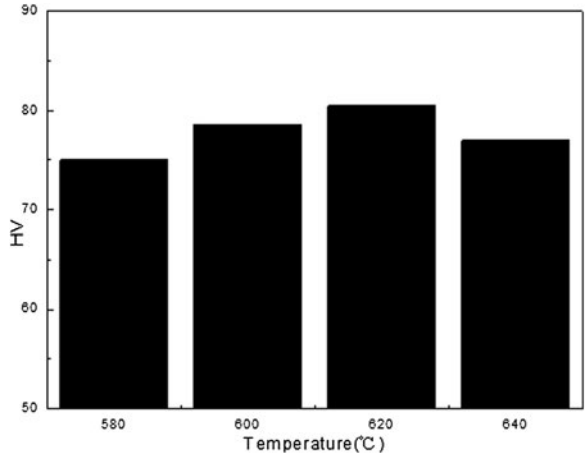

FIG. 11. Vickers hardness chart of ZL104 experimental alloy treated at different pouring temperatures.

kinds of metal components were produced by rolling-casting process. The surface of metal component quality was good; the tensile strength of ZL104 metal components is shown in Fig. 10. Therefore, the most tensile strength is the metal components produced with the rolling-casting temperature at 620 °C and velocity of plate at 10 cm/s. Obviously, the pouring temperature at 620 °C and the substrate speed at 10 cm/s could maintain the balance of melting and solidification of the material.

Figure 11 is the comparison figure of four kinds of samples preparation for SRCM with different pouring temperatures. The vickers analysis sample of hardness is made in the same place of the samples. From the figure it can be seen that the average vickers hardness of five position in per sample is more than 65 HV. The largest average vickers hardness is 81.55 HV, which is obtained at pouring temperature of 620 °C. According to the data of the samples, the highest vickers hardness is located in the center of sample. It can be concluded that refinement of particles could increase material strength significantly, but the segregation of microstructure could decrease material strength.

IV. CONCLUSIONS

(1) ZLl04 alloy was produced by SRCM, through which is the primary dendritic crystal is easily crushed due to the narrow and space, resulting in fine grains. The paper studied the influences of parameters, such as effect by the velocity of plate and temperature gradient on the microstructure evolution and mechanical property of ZLl04 alloy by SRCM.

(2) The synchronous rolling-casting mass force produced with uniform metal slurry by substrate movement could contribute to grain refinement in the process. The microstructure and mechanical performance is excellent when the pouring temperature is at

620 °C and the velocity of plate is at 10 cm/s, the tensile strength and elongation of the ZL104 alloy reached 211.89 Mpa and vickers hardness reached 81.5, average roundness reached 2.2, and average grain size reached 41.15 μm.

ACKNOWLEDGMENTS

Special thanks should go to Prof. Chen Guangnan who provided lots of academic help for this paper. This paper is funded by the National Natural Science Foundation of China (No. 51341009).

REFERENCES

1. E. Barnett and C. Gosselin: Weak support material techniques for alternative additive manufacturing materials. *Addit. Manuf.* **8**, 95–104 (2015).
2. B.N. Turner and S.A. Gold: A review of melt extrusion additive manufacturing processes: II. Materials, dimensional accuracy, and surface roughness. *Rapid Prototyping J.* **21**, 250 (2015).
3. B.N. Turner, R. Strong, and S.A. Gold: A review of melt extrusion additive manufacturing processes: I. Process design and modeling. *Rapid Prototyping J.* **20**, 192 (2014).
4. F.M. Mazzolani: 3D aluminium structures. *Thin Wall Struct.* **61**, 258 (2012).
5. M. Orme: On the genesis of droplet stream microspeed dispersions. *Phys. Fluids A* **3**, 2936 (1991).
6. C.S. Rice, P.F. Mendez, and S.B. Barown: Metal solid freeform fabrication using semi-solid slurries. *JOM* **52**, 31 (2000).
7. J.D. Williams and C.R. Deckard: Advances in modeling the effects of selected parameters on the SLS process. *Rapid Prototyping J.* **4**, 90 (1998).
8. S. Kumar: Selective laser sintering: A qualitative and objective approach. *JOM* **55**, 43 (2000).
9. D.R. Smalley and C.W. Hull: Method of making a three dimensional object by stereolithography. US Patents, US 07/429,435, 1992.
10. J. Gardan: Additive manufacturing technologies: State of the art and trends. *Int. J. Prod. Res.* **1**, 1605–1615 (2015).
11. J. Sun, W. Zhou, D. Huang, J.Y. Fuh, and G.S. Hong: An overview of 3D printing technologies for food fabrication. *Food Bioprocess Technol.* **1**, 3118–3132 (2015).
12. T. Monaghan, A.J. Capel, S.D. Christie, R.A. Harris, and R.J. Friel: Solid-state additive manufacturing for metallized optical fiber integration. *Composites, Part A* **76**, 181 (2015).
13. H.P. Tang, G.Y. Yang, W.P. Jia, W.W. He, S.L. Lu, and M. Qian: Additive manufacturing of a high niobium-containing titanium aluminide alloy by selective electron beam melting. *Mater. Sci. Eng., A* **636**, 103 (2015).
14. L. Yang, O. Harrysson, H. West, and D. Cormier: Mechanical properties of 3D re-entrant honeycomb auxetic structures realized via additive manufacturing. *Int. J. Solids Struct.* **69–70**, 475 (2015).
15. Z.M. Shi, Q. Wang, G. Zhao, and R.Y. Zhang: Effects of erbium modification on the microstructure and mechanical properties of A356 aluminum alloys. *Mater. Sci. Eng., A* **626**, 102 (2015).
16. C.G. Kang, J.S. Choi, and K.H. Kim: The effect of strain rate on macroscopic behavior in the compression forming of semi-solid aluminum alloy. *J. Mater. Process. Technol*. **88**, 159 (1999).
17. M.C. Flemings: Behavior of metal alloys in the semisolid state. *Metall. Mater. Trans. B* **22**, 269 (1991).
18. S.D. Kumar, A. Mandal, and M. Chakraborty: Solid fraction evolution characteristics of semi-solid A356 alloy and in-situ A356-TiB_2 composites investigated by differential thermal analysis. *Int. J. Miner. Metall. Mater.* **22**, 389 (2015).